Microelectronic Engineering 157 (2016) 24–30

Contents lists available at ScienceDirect

Microelectronic Engineering

journal homepage: www.elsevier.com/locate/mee

Double side polydimethylsiloxane gradient gratings as vectorial displacement sensing elements

Hao Guo, Jun Tang *, Kun Qian, Miaomiao Zhao, Jiangtao Yang, Wei Zhang, Binzhen Zhang, Jun Liu *, Chenyang Xue, Wendong Zhang

Science and Technology on Electronic Test & Measurement Laboratory, North University of China, Taiyuan, Shanxi 030051, China

ARTICLE INFO

Article history:
Received 6 November 2015
Received in revised form 26 January 2016
Accepted 8 February 2016
Available online 10 February 2016

Keywords:
Vectorial displacement
Gradient gratings
Double side PDMS
Sensing element

ABSTRACT

In this work, an orthogonal optical grating structure is demonstrated as a displacement sensing element. The grating is made with gradient periodicity and height on both sides of a polydimethylsiloxane (PDMS) substrate using an oxygen plasma treatment of prebent PDMS. Based on Fraunhofer diffraction effect, it is experimentally shown that any displacement can be quantitatively characterized in both the *x* and *y* directions with an estimated maximum error value of 0.4% and a resolution of 300 μm^{-1}. With this simple and low cost technology, it is proved that this structure can operate as a single element sensor for vectorial displacement signals, which can be applied for vectorial displacement measurement and multi-axis integrated displacement sensors.

1. Introduction

Vectorial displacement sensors, which are capable of high-resolution and sensitivity to measure the movement position and direction for the target object, have a wide variety of applications including aerospace [1], precision equipment [2], vibration monitoring [3], health monitoring [4], and safety monitoring [5]. In order to improve the chip integration and reduce the size and cost, many methods, materials, technology and algorithms have been proposed [6,7].

To achieve the vectorial displacement measurement, the main technology used was assembly of the element in multiple directions. Wang [8,9] reported a Single-Electrode-Based Sliding triboelectric nanogenerator for self-powered displacement vector sensor system. Two similar nanogenerators were assembled in the *x* and *y* direction to detected the vectorial information. However, the errors generated in the process of assembling two or more of sensitive elements, the complexity of the processes, and the relatively large size are limiting their application in engineering practice.

In the literature, others are using structure decoupling. Izhar [10] reported a low power thermally actuated bi-axis Silicon-On-Insulator (SOI) micromirror to perform optical coherence tomography (OCT) system with high angular displacements and vertical displacements. However, the complicated micro/nano manufacturing and packaging processes restricted its development.

In this paper, we demonstrate a vector displacement sensing method using a single element, which was fabricated by oxygen plasma technology to form an orthogonal gradient optical grating structure on both sides of a Polydimethylsiloxane (PDMS) substrate which was pre-bent as a shape of ellipse. The sample moved in the path of these increasing periodicity structures, results in a movement of the diffractive spot created by a laser beam. Using this structure, the displacement of sample has been quantitatively characterized in both the *x* and *y* directions to estimate the vectorial information of displacement with an error of 0.4% and a resolution of 300 μm^{-1}. It represents a tendency towards practical application of single-chip integrated vector sensor systems.

2. Materials and methods

The sinusoidal morphology with gradient periodicity of optical grating was formed on PDMS films. The PDMS films were prepared by mixing 12 g of pre-polymer (Sylgard184 from Dow Corning) with a curing agent in a 10:1 ratio using a spin coating process and cured at 65 °C for 30 min in the clean room. The schematic (Fig. 1) shows the steps followed to prepare a square double-side orthogonal gradient grating structure with thickness of about 1 mm and side length 20 mm.

As shown in Fig. 1, the PDMS sample was first prepared on a PET film, which was used then as structural support and guarantees

* Corresponding authors.
E-mail addresses: tangjun@nuc.edu.cn (J. Tang), liuj@nuc.edu.cn (J. Liu).

http://dx.doi.org/10.1016/j.mee.2016.02.010
0167-9317/© 2016 Published by Elsevier B.V.

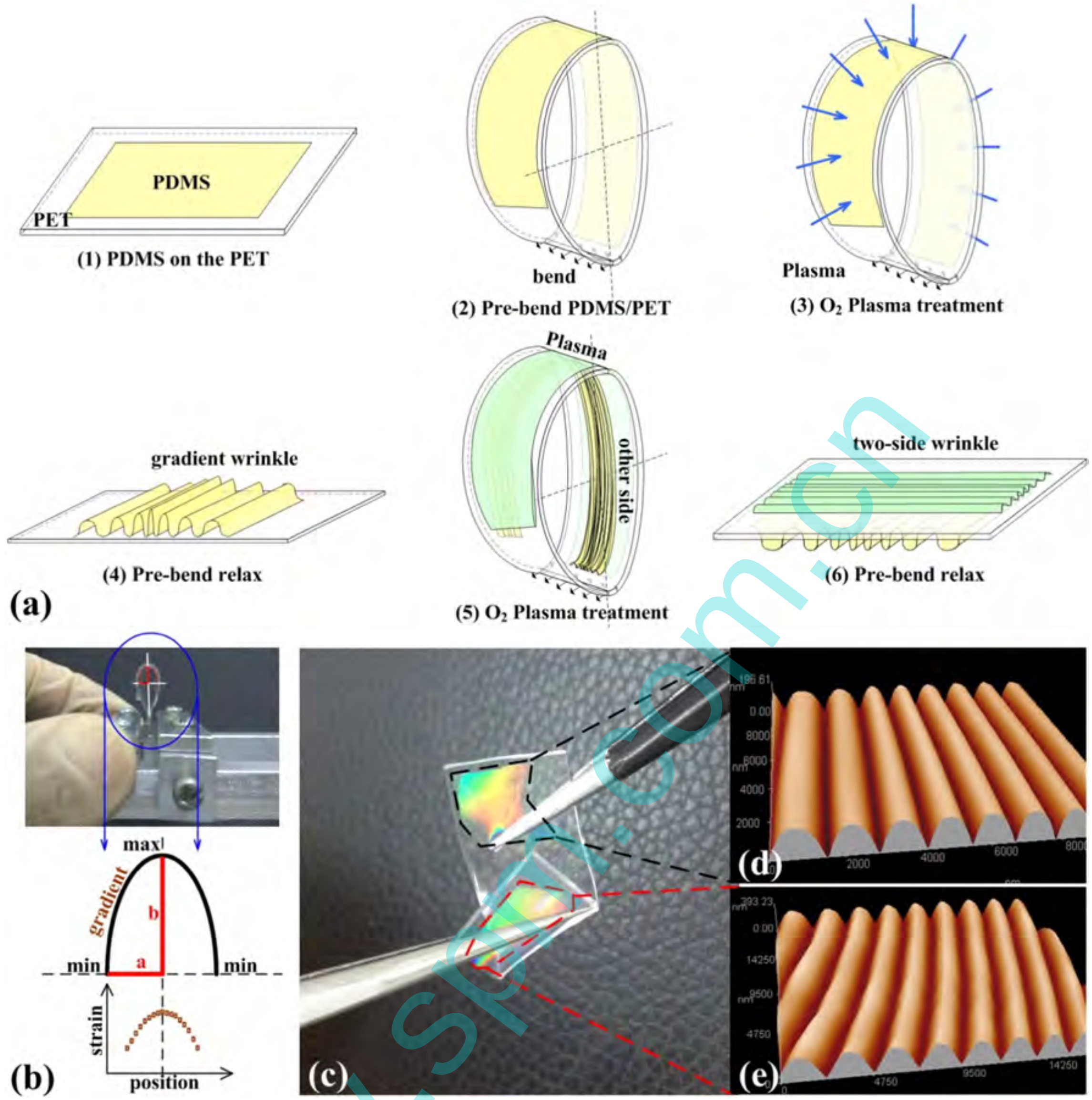

Fig. 1. PDMS grating fabrication and characterizations. (a) Schematic diagram of the fabrication process of double-side orthogonal gradient grating structure on the surface of PDMS. In step 5 PDMS was turned by 90°. (b) PDMS substrate pre-bent in an oval shape to create a strain gradient on the surface of PDMS. (c) Optical image. (d) & (e) AFM image of grating structure for both sides.

PDMS flatness during and after processing. The PDMS sample was first pre-bent to take the shape of an ellipsoid (shown in Fig. 1a(2)) and then treated using oxygen plasma to form wrinkled SiO_x layers on the surface the PDMS substrate (IoN Wave 10, PVA-TePla, Germany), which have been reported in our previous works [11,12]. The same method was also used on the other side of the PDMS with an angle difference of 90°, forming the orthogonal gradient grating structures on both sides of the PDMS, as shown in Fig. 1c.

The surface geometry of the grating arrays were characterized using atomic force microscopy (AFM, CSPM5000, Being Nano-Instrument Ltd., China) and a gradually increasing periodicity on both sides of PDMS was achieved as shown in Fig. 1d, e, due to the gradient strain distribution on the surface PDMS substrate, which was pre-bent as ellipsoid as shown in Fig. 1b.

A 532 nm laser (Cobolt 04-01, Cobolt, Sweden) was used as the laser source. The diffracted spots were projected on a black screen. The image was taken by a CCD (E-M1, Olympus Corporation, Japan), as shown in Fig. 2e.

3. Results and discussions

3.1. Orthogonal gradient PDMS grating and characterization

The fabrication process was presented in Fig. 1, and the corresponding model was shown in Fig. 1(b). The pre-bent substrate takes the shape of an ellipsoid with *a* being the minor axis and *b* being the long axis. This bending scheme forms a gradient strain distribution on the surface of the PDMS substrate. Due to the gradient strain and by controlling the side on which the plasma treatment was applied, a gradually increasing periodicity (starting from approximately (2 ± 0.1) μm) on both sides of PDMS was achieved as shown in Fig. 1d, e. Desired periodicity of the gratings can be calculated as introduced in our previous studies [12,13].

The double-sided gradient PDMS grating was fixed to a translation stage to perform the displacement characterization as shown in Fig. 2e. The sample was moving by controlling the micro-meter located on the controller with a step of 10 μm along or across the grating direction.

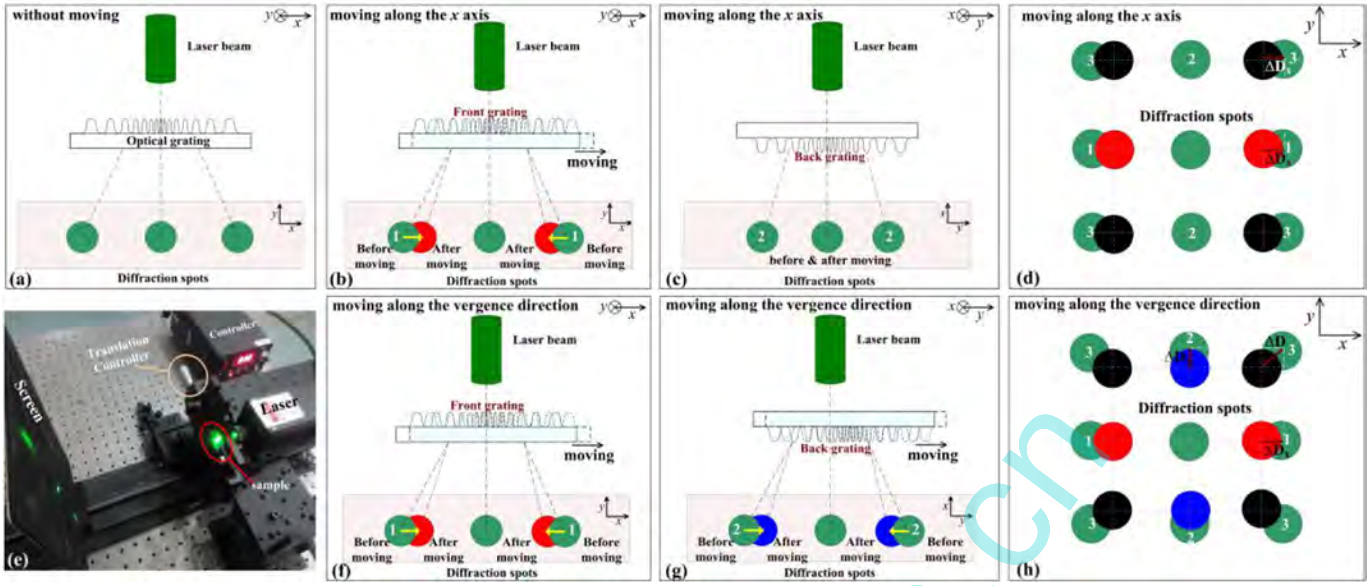

Fig. 2. The diffraction spot movement characterizations. (a) Optical diffraction without moving the sample (b & c) The spot '1' & '2' moving as a function of different grating periodicity under the moving sample along the x axis, and the correspond diffraction spot moving as shown in (d). (e) The optical measurement setup (f & g) The spots '1' & '2' moving as a function of different grating periodicity under moving the sample along the vergence direction (h) The diffraction spot moving as a function of different grating periodicity under the moving sample along the vergence direction.

As shown in Fig. 2a, d, the first-order diffraction spot was distributed as nine positions indicated by the green spot. With moving the sample along the x axis, the spot was moving close to the center due to the increasing periodicity based on the theory of multi-slit Fraunhofer diffraction, thus resulting in shown in Fig. 2d.

Attributing to the orthogonal gratings on the two sides surface of PDMS, the sample was moving along the grating direction on one side and perpendicular to the grating on the other side. As shown in Fig. 2b–d, with moving along the x axis (which perpendicular to the front grating direction but along the back grating direction), two phenomena occur, the spots '1' were moving close to the center as shown the red spots in the Fig. 2d due to the increasing gradient periodicity. However, the spots '2' were not moving due to the back grating direction was the same direction to the moving direction (x axis as shown in Fig. 2c) and the periodicity was uniform. Spots '3', moved in a more complex way as indicated by the black spots in Fig. 2d, h. The spots '3' have a composite movement that is the resultant of movements of the spots '1' and '2' indicated by the black spots in Fig. 2h. Moving along the diagonal direction, the two side gratings formed an angle to the displacement direction. The spots '1' and '2' were moving close to the center due to the increasing periodicity for grating on both sides of the PDMS substrate, as shown in Fig. 2f, 2g. Here, the movement of spots '3'(indicated by the black spots) is a function of spot '1' and '2' movements and spots '3' are moving along the diagonal direction which can be composed from the movement along the x axis and y axis.

To quantitatively characterize the displacement performance of the gradient double-sided PDMS gratings, the home-made characterization system shown in Fig. 2e was used to analyze the diffraction laser spot images, as shown in Figs. 3 and 4. In this work, the sample was moving along the x axis, thus being perpendicular to the direction of the grating on the front side, parallel to the direction of the back side grating.

3.2. Displacement calculation method

Both the movement and the intensity variations of the laser spots were estimated by the processing using MATLAB software under moving the sample. The intensity distributions of the diffracted laser spots and the positions of these laser spots '1', '2' and '3' can all be calculated to study the characteristics of displacement using this method.

Fig. 4 shows the movement of the diffracted laser spot. By moving the sample along the x axis, the center spot was always maintained its position, but the eight surrounding spots moved as described below. As shown in Fig. 4a–h, the spots '1' were formed due to diffraction from the perpendicular to the moving direction on the front side, while the spots '2' were formed due to diffraction from the parallel to the moving direction on the back side. Especially, the spots '3' were formed due to diffraction from the spots '1' and '2'. The spots '1' were moved closer to the central spot attribute to the increased grating periodicity on this side. However, the spots '2' were not moved due to the uniform periodicity. The movement of spots denoted by '3' embraces the movement information of both spots '1' and '2'. In addition, the intensities of all laser spots decreased with increasing strain.

The periodicity and height of the grating can be quantitatively calculated as follows [14–16]:

$$b = \lambda\sqrt{\left(\frac{L}{S}\right)^2 + 1} \tag{1}$$

where b is the value of grating periodicity, the laser wavelength λ is 532 nm, S is the distance between the zero-order and first-order diffraction spots, and the distance L between the sample and the screen is 10 cm.

The height h of the grating versus the grating periodicity being given by:

$$h = \frac{b(1 - \cos\alpha)}{2\sin\alpha} \tag{2}$$

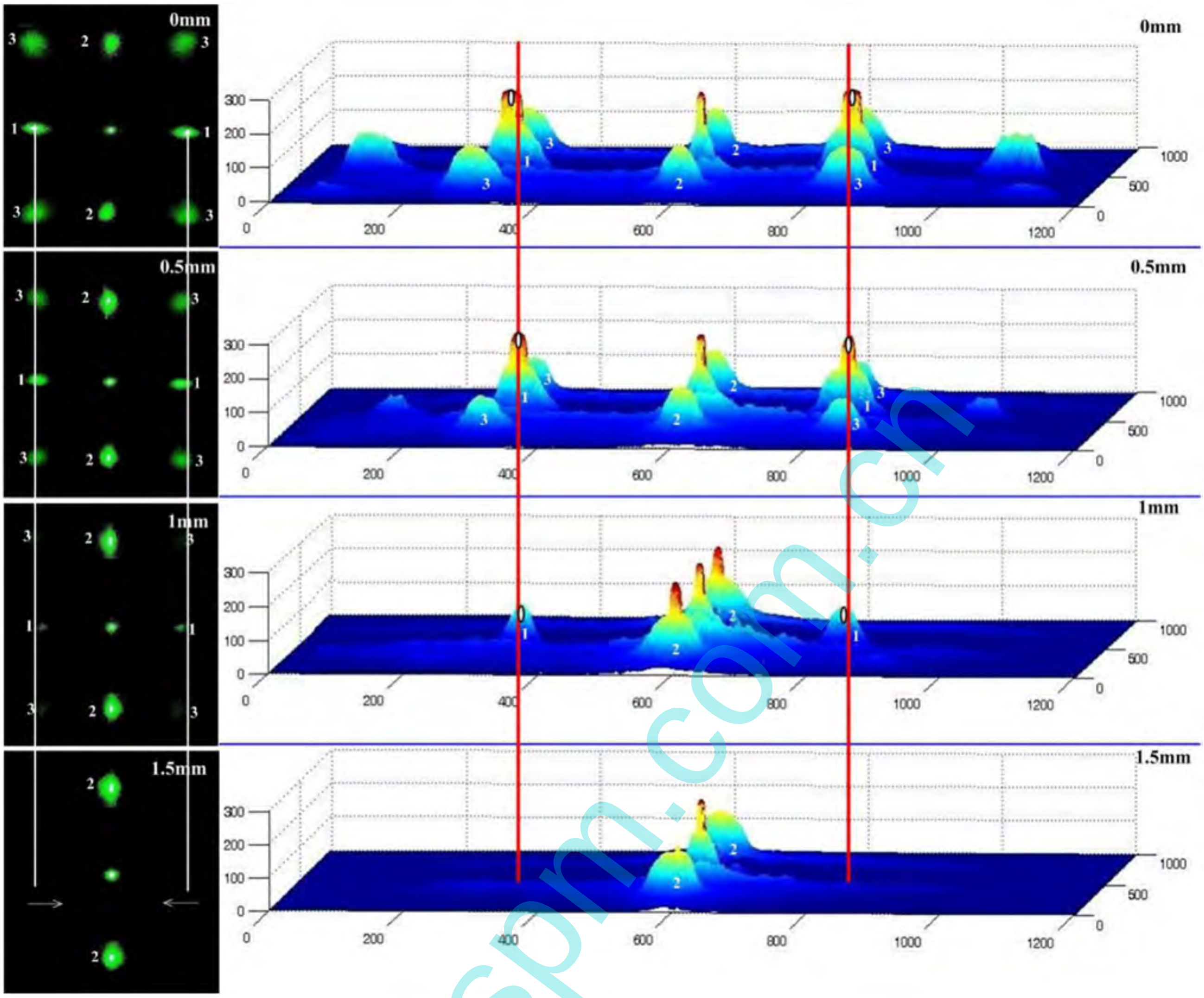

Fig. 3. Calculation of displacement of sample from the diffracted laser spot using MATLAB.

$$\frac{\sin\alpha}{\alpha} = \frac{b}{C} \tag{3}$$

Where, b is the modified grating periodicity, C the length of sample being 20 mm, 2α is the curved radian of the grating.

Meanwhile, the intensity can be calculated by [14–16]:

$$I = \sum_{q=-\infty}^{\infty} N^2 {J_q}^2\left(\frac{h}{2}\right)\left[\frac{\sin\left(\frac{N\pi}{\lambda}\times\left(\sin\beta-\frac{q\lambda}{b}\right)\right)}{\frac{N\pi}{\lambda}\times\left(\sin\beta-\frac{q\lambda}{b}\right)}\right]^2 \tag{4}$$

$$\mathrm{M} = \left[\frac{\sin\left(\frac{\mathrm{N}\pi}{\lambda}\times\left(\sin\beta-\frac{\mathrm{q}\lambda}{b}\right)\right)}{\frac{\mathrm{N}\pi}{\lambda}\times\left(\sin\beta-\frac{\mathrm{q}\lambda}{b}\right)}\right] \tag{5}$$

where, $\mathrm{J_q}(\frac{\mathrm{h}}{2})$ is the first kind Bessel function [17], q is the diffraction grades, h is the height of grating, N is the number of gratings, β is the diffraction angle, M is the diffraction factor, which is used to point out the location of the diffraction spot.

The grating periodicity and height were calculated using Eqs. (1)–(3), as shown in Fig. 5a. The gradient periodicity was increasing from 2 μm to 2.41 μm for both sides of PDMS, and the height was reduced from the 0.6 μm to 0, which resulted in the diffraction spots disappearance.

For the front grating (for the spots ‘1’), along the displacement direction (x axis), an increasing periodicity is met in the path of movement. The spots ‘1’ moved 5 mm with a displacement of 1.75 mm as shown in Fig. 5b. Meanwhile, the intensity disappeared as the height tends to zero. However, for the back grating (for the spots ‘2’) because it was oriented in parallel to the moving direction, there was not any periodicity variation in the path of movement direction, resulting in no movement for the spots ‘2’ as shown in Fig. 5c. Spots ‘3’ movement was composed from spots ‘1’ and ‘2’ movement as a result of the displacement and intensity of spots ‘1’ and ‘2’ as shown in Fig. 5d. These phenomena offer a potential method for vectorial displacement using a single element by calculating the variables of spots ‘1’ and ‘2’ using the spots ‘3’, where the spots ‘1’ and ‘2’ represent movement along as the x and y axis correspondingly.

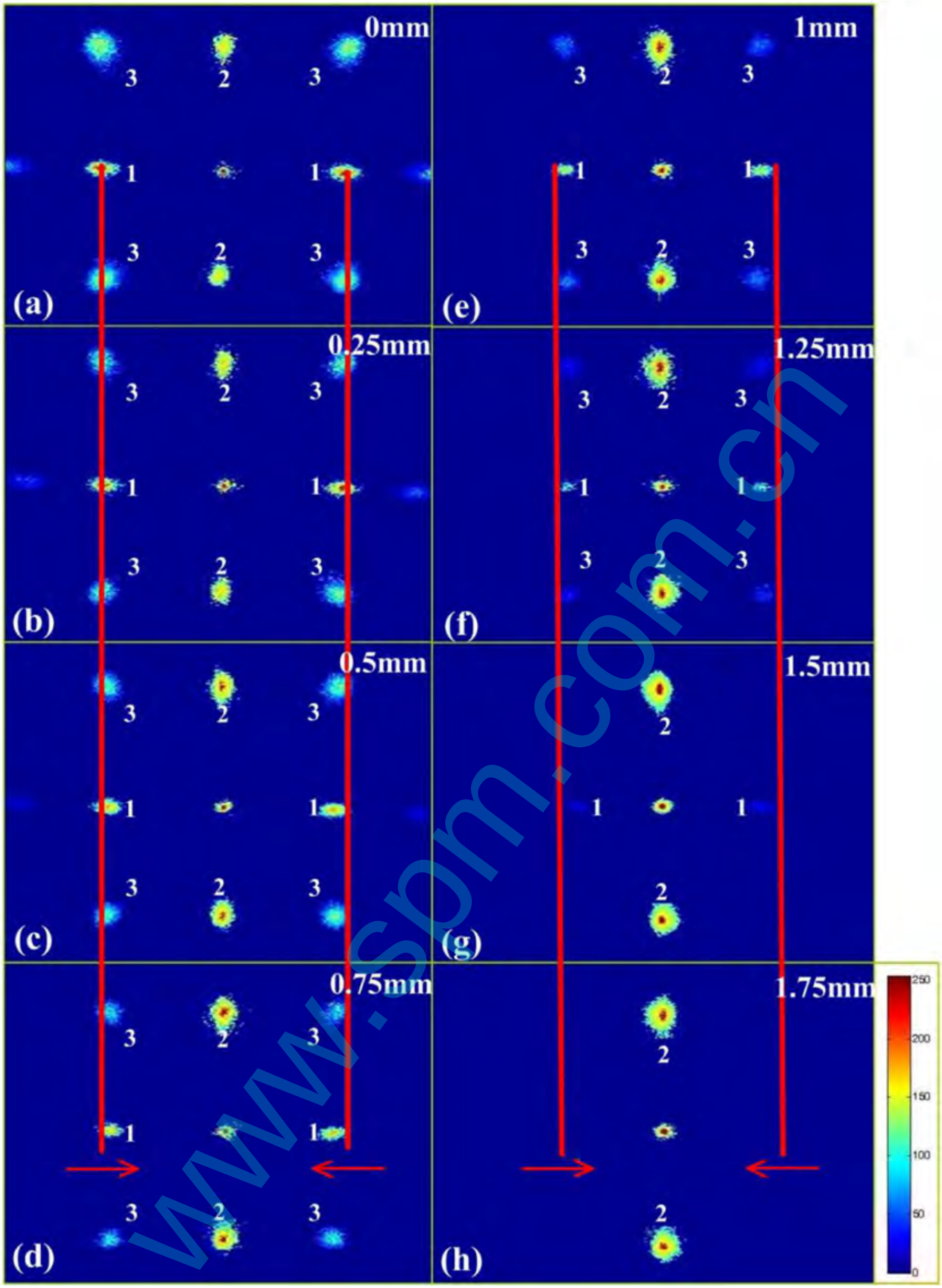

Fig. 4. Photographs of laser diffractions through the double-side orthogonal gradient grating with moving sample along the *x* axis.

Similarly, the results can also be verified by an intensity test. As shown in Fig. 5, clear and same reduction of the intensities of spots '1' and '3' was observed. And there was no any changes for the intensity of spots '2'.

3.3. Vectorial displacement performance characterization

Using the methods described above, the vectorial displacement performance was then characterized using the three types of spots. All samples, equipment and the control system described above were used to study methods of vectorial displacement sensing.

Fig. 2h shows a schematic diagram in the case as moving the sample along the vergence direction, spots '1' and '2' have moved close to center spots along the *x* and *y* axis, resulting in further movement of spots '3', which can be more sensitive for displacement sensing. The displacement of the spots '3' was denoted by ΔD, and can be analyzed to the *x* and *y* components denoted by ΔD_x and ΔD_y

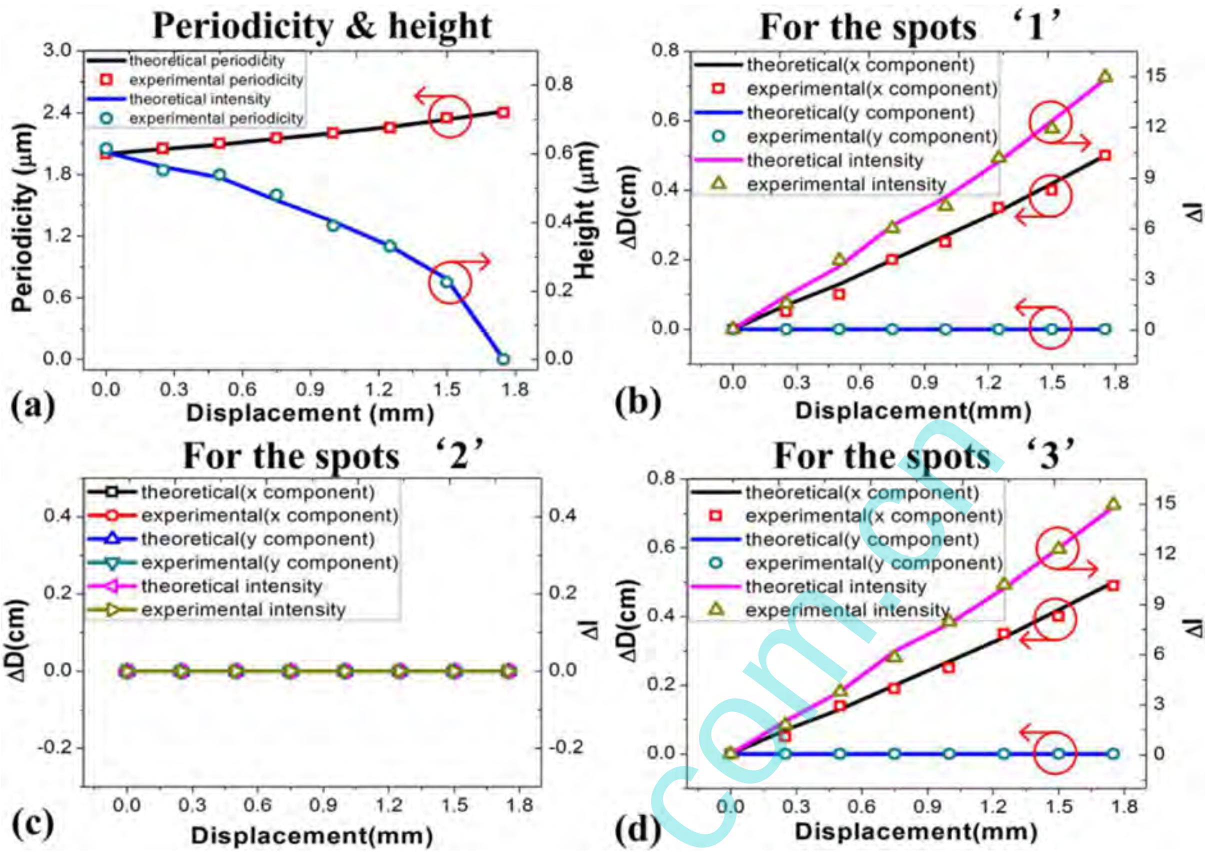

Fig. 5. The optical diffraction characterizations for three types of spot under moving sample along the *x* axis. (a) Strain induced grating periodicity and height variations on the two sides of substrate. (b) Strain induced displacement and intensity variations of spot '1'. (c) Strain induced displacement and intensity variations of spot '2'. (d) Strain induced displacement and intensity variations of spot '3'.

respectively which depend from the direction and the magnitude of the displacement. The variations in the spots '3' embrace vectorial information about the displacement. The magnitude of displacement can be calculated as:

$$\Delta D = \begin{cases} \Delta D_y arcsin\theta \\ \Delta D_x arccos\theta \end{cases} \tag{6}$$

The direction can be calculated as:

$$\theta = \arctan\left(\frac{\Delta D_y}{\Delta D_x}\right) \tag{7}$$

Where, ΔD is the displacement, ΔD_x and ΔD_y are the displacement components along the *x* and *y*, respectively, θ is the angle between the vergence direction and grating direction (shown in Fig. 6a).

To prove the feasibility of our methods we have moved the sample along θ = 45° to the grating. The eight surrounding spots change position as a function of the vectorial displacement. The spots '3' move along the direction of the displacement and the variable have been defined as 'ΔD' in red font, and the *x* and *y* components have been calculated to be ΔD_x and ΔD_y respectively, as shown in Fig. 6a.

The displacement and intensity of spots '3' can be used to calculate the magnitude and direction of the movement for the sample. The ΔD_x and ΔD_y components of the displacement have been calculated using MATLAB software, as shown in Fig. 6a. The direction of the strain was calculated to be approximately 45° using Eqs. (1) & (7), as shown in Fig. 6h. Also, the magnitude can be calculated using Eq. (6) and the resolution was about 300 μm^{-1} using the displacement of spots and about 116 μm using the intensity of spots with the max errors was about 0.4%. The measurement results show quite good agreement with the theoretical results. Therefore, this method has been successfully used to sense vectorial displacement signals using a single element.

The method was based on the movement of diffraction spots, which was based on the gradient periodicity grating. In this work, due to the controllable ellipsoidal bending and plasma parameters, the periodicity gradient on the sensing element was stable and reproducible.

4. Conclusion

In summary, using oxygen plasma, on both sides of a pre-bent to an ellipsoid shape PDMS substrate, orthogonal optical grating structures were formed with increasing periodicity and reducing height. The displacement and intensity of diffraction spots have been characterized in both the *x* and *y* directions and can give the magnitude and direction for the displacement of the sample by using an algorithm based on the Fraunhofer diffraction effect. With an estimated maximum error of 0.4% and a resolution of 300 μm^{-1}, this method can be used as a single element sensor for vectorial displacement estimation.

Acknowledgments

We acknowledge the financial support from the Natural Science Foundation of China (51225504, 61571406 and 91123036), program for the top young academic leaders of higher learning Institutions of Shanxi.

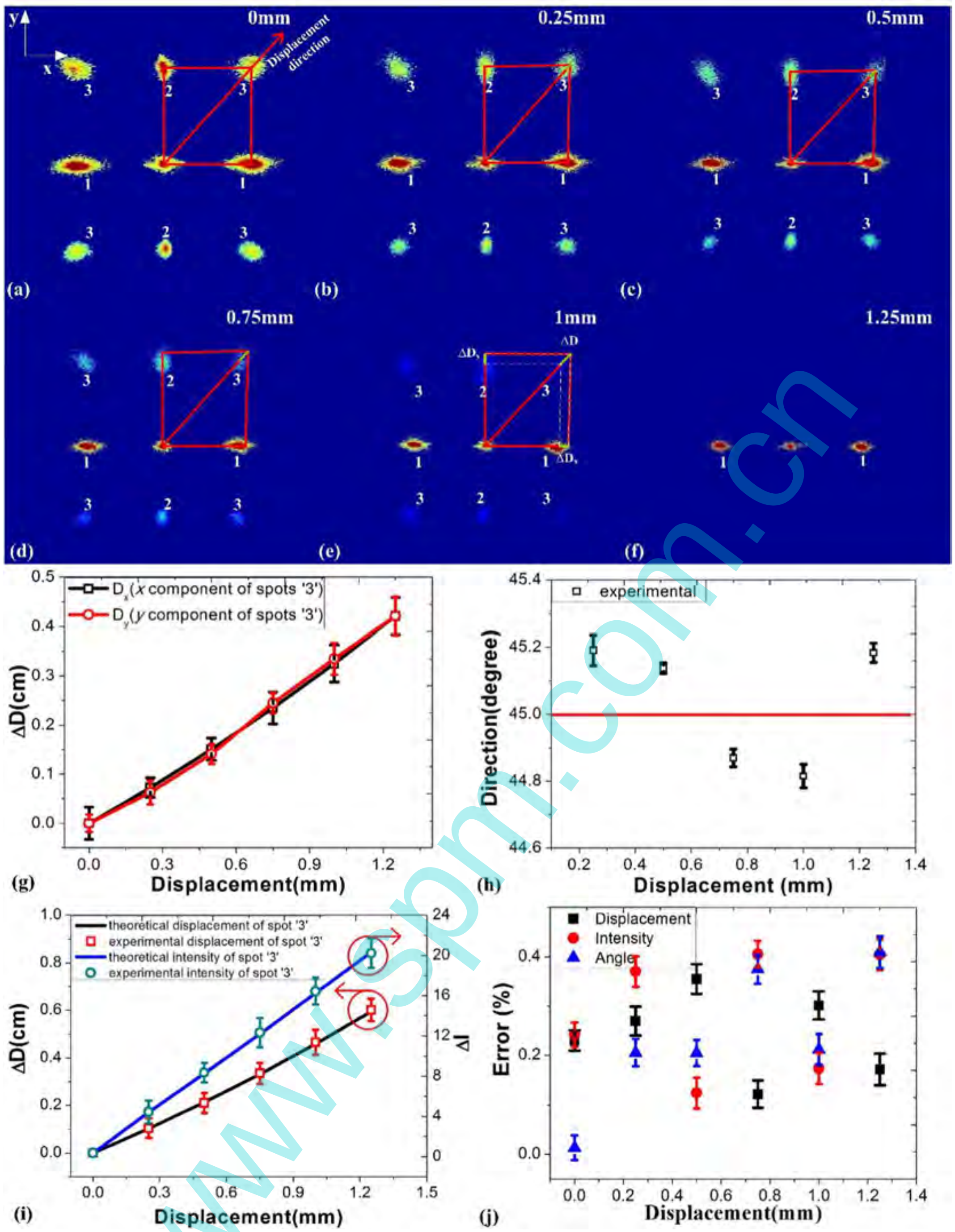

Fig. 6. Vectorial displacement characterizations under the sample moving along a 45° angle. (a–f) The spot displacement versus the movement of the sample along the 45° direction. (g) The *x* component and *y* components of displacement for the spot '3' under moved the sample. (h) The angle direction of the moved sample. (i) Displacement and intensity variations for moved sample (j) the corresponding calculated error. (For interpretation of the references to color in this figure legend, the reader is referred to the web version of this article.)

References

[1] V.G. Welsby, Nature 218 (1968) 890–891.
[2] K. Kristiansen, P. McGuiggan, G. Carver, C. Meinhart, J. Israelachvili, Langmuir 24 (4) (2008) 1541–1549.
[3] C. Baker, L. Chen, X. Bao, Opt. Express 23 (14) (2015) 17838–17844.
[4] J.N. Dash, R. Jha, J. Villatoro, S. Dass, Opt. Lett. 40 (4) (2015) 467–470.
[5] T.W. Ng, Sensors Actuators A 107 (2003) 21–25.
[6] T. Iwasaki, T. Takeshita, Y. Arinaga, S. Takeuchi, M. Furue, E. Higurashi, R. Sawada, K. Uemura, H. Ando, Sensors Actuators A 221 (2015) 1–8.
[7] C. Braunsmann, V. Prucker, T.E. Schaffer, Appl. Phys. Lett. 104 (10) (2014) 103101.
[8] Y. Yang, H. Zhang, J. Chen, Q. Jing, Y.S. Zhou, X. Wen, Z.L. Wang, ACS Nano 7 (8) (2013) 7342–7351.
[9] Q.S. Jing, Y.N. Xie, G. Zhu, R.P.S. Han, Z.L. Wang, Nat. Commun. 6 (2015) 8031.
[10] U. Izhara, A.B. Izharb, S. Tatic-Lucica, Sensors Actuators A 167 (2011) 152–161.
[11] Y. Yang, X. Han, W.L. Ding, S.C. Jiang, Y.P. Cao, C.H. Lu, Langmuir 29 (23) (2013) 7170–7177.
[12] J. Tang, H. Guo, M. Chen, J. Yang, D. Tsoukalas, B. Zhang, J. Liu, C. Xue, W. Zhang, Sci. Rep. 5 (2015) 16527.
[13] J. Tang, H. Guo, M. Zhao, J. Yang, D. Tsoukalas, B. Zhang, J. Liu, C. Xue, W. Zhang, Sensors Actuators B 218 (2015) 145–151.
[14] M. Nania, O.K. Matar, J.T. Cabral, Soft Matter 11 (15) (2015) 3067–3075.
[15] B. Li, T. Du, B. Yu, J. Gucht, F. Zhou, Small 12 (28) (2015) 3494–3501.
[16] Topuzoski, Opt. Commun. 330 (2014) 184–190.
[17] T.A. Planchon, L. Gao, D.E. Milkie, M.W. Davidson, J.A. Galbraith, C.G. Galbraith, E. Betzig, Nat. Methods 8 (2011) 417–423.